Journal of Power Sources 236 (2013) 33–38

Contents lists available at SciVerse ScienceDirect

Journal of Power Sources

journal homepage: www.elsevier.com/locate/jpowsour

Short communication

# Synthesis and electrochemical performance of $LiVO_3$ cathode materials for lithium ion batteries

X.M. Jian, J.P. Tu*, Y.Q. Qiao, Y. Lu, X.L. Wang, C.D. Gu

*State Key Laboratory of Silicon Materials, Key Laboratory of Advanced Materials and Applications for Batteries of Zhejiang Province and Department of Materials Science and Engineering, Zhejiang University, Hangzhou 310027, China*

## HIGHLIGHTS

- $LiVO_3$ is synthesized by a ball-milling route followed by a solid-state reaction.
- The $LiVO_3$ compound synthesized at 350 °C possesses the optimal performance.
- It delivers an initial discharge capacity of 302.5 mAh $g^{-1}$.
- Li-ion diffusion coefficient of $10^{-9.5}$–$10^{-8}$ $cm^2$ $s^{-1}$ is calculated by GITT.

## ARTICLE INFO

*Article history:*
Received 21 October 2012
Received in revised form
30 January 2013
Accepted 2 February 2013
Available online 26 February 2013

*Keywords:*
Lithium metavanadate
Diffusion coefficient
Lithium ion battery
Cathode

## ABSTRACT

$LiVO_3$ is synthesized via a ball-milling route followed by a solid-state reaction at different temperatures. As cathode materials for lithium ion batteries, the electrochemical performances of $LiVO_3$ are investigated by galvanostatic charge–discharge test and electrochemical impedance spectroscopy (EIS). The $LiVO_3$ compound synthesized at 350 °C possesses the optimal performance, delivering an initial discharge capacity of 302.5 mAh $g^{-1}$ between 1.0 V and 3.5 V at a current density of 50 mA $g^{-1}$, and exhibiting a good cycling stability. Li-ion diffusion coefficient of $10^{-9.5}$–$10^{-8}$ $cm^2$ $s^{-1}$ in the $LiVO_3$ electrode is calculated by galvanostatic intermittent titration technique (GITT). The good performances can be attributed to its relatively low crystallization and small particle size.



## 1. Introduction

Nowadays lithium ion batteries have been applied in a wide variety of ways owing to their high energy density and long cycle life. They have been considered to be promising energy storage devices for hybrid electric vehicles (HEV) and electric vehicles (EV). Since the first commercial lithium ion battery was developed by researchers at Sony Energytech in the late 1980s [1], much effort has been taken to seek for alternative cathode materials with high capacity and low cost. The vanadium oxides and vanadium derivatives have been considered to be one of the most promising candidates [2–4]. Among these vanadium derivatives, the layered $LiV_2O_5$ [5–8] and $LiV_3O_8$ [9–12] are researched mostly. But it is difficult to synthesize $LiV_2O_5$ for it has two different valence states of vanadium ($V^{5+}$ and $V^{4+}$). While $LiV_3O_8$ faces a serious capacity fading problem during the lithium ion intercalation and deintercalation processes.

V. Pralong et al. [13] firstly put forward that the $LiVO_3$ compound can be used as a cathode material. Although it possesses a relatively low voltage, easy synthesis and a high specific capacity still make it a promising candidate as a cathode material. It belongs to space group C2/c [14], and has a unidimensional character of its structure built up of chains of corner sharing $VO_4$ tetrahedra, interconnected through $LiO_6$ octahedra. There exists the possibility of structure rearrangement during the lithium ion intercalation. After the first intercalation process, it transforms into a Li-rich rock salt structured $Li_2VO_3$, which belongs to space group Fd-3m and is stable during cycling process. Up to now, there are lots of methods to synthesize vanadium oxides and vanadium derivatives, such as solid-state reaction [15–17], sol–gel [18–21], combustion [22–24], spray drying [25–27], hydrothermal [7,28,29] and rheological phase reaction methods [30]. Traditional solid-state reaction is considered to be the simplest way to synthesize the cathode materials.

* Corresponding author. Tel.: +86 571 87952856; fax: +86 571 87952573.
*E-mail addresses:* tujp@zju.edu.cn, tujplab@zju.edu.cn (J.P. Tu).

0378-7753/$ – see front matter © 2013 Elsevier B.V. All rights reserved.
http://dx.doi.org/10.1016/j.jpowsour.2013.02.004

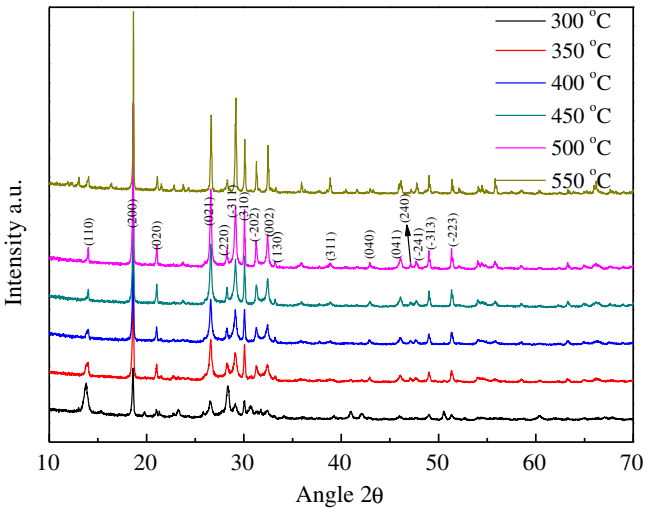


**Fig. 1.** XRD patterns of $LiVO_3$ powders synthesized at different temperatures: (a) 300 °C; (b) 350 °C; (c) 400 °C; (d) 450 °C; (e) 500 °C; (f) 550 °C.

In this present work, the $LiVO_3$ compound was synthesized via a simple ball-milling route followed by a solid-state reaction at low temperatures. The structure and electrochemical properties of this material synthesized at different temperatures were investigated.

## 2. Experimental

The $LiVO_3$ materials were synthesized using a balling route followed by a solid state reaction. $Li_2CO_3$ and $NH_4VO_3$ were used as raw materials. Stoichiometric $Li_2CO_3$ and $NH_4VO_3$ were ball-milled using ethanol as solvent at room temperature in air. After evaporating the ethanol, the precursor was ground using mortar and pestle. At last the powder was calcined at temperatures ranging from 300 to 550 °C in air for 12 h to yield the final products. The structures and morphologies of the powders were characterized by X-ray diffraction (XRD, Philips PC-APD with Cu Kα radiation) and scanning electron microscopy (SEM, HITACHI SU70).

The working electrode was prepared by a slurry coating procedure. The slurry consisted of 75 wt. % $LiVO_3$ powder, 20 wt. % carbon conductive agent and 5 wt. % polyvinylidene fluoride (PVDF) as a binder was coated on aluminum foil. After drying in an oven at 90 °C for 24 h, the sample was pressed under a pressure of 20 MPa. A metallic lithium foil was used as anode, 1 M $LiPF_6$ in ethylene carbonate (EC)–diethyl carbonate (DEC) (1:1 in volume) as the electrolyte and polypropylene microporous film (celgard 2300) as separator. The CR2025 coin-type cells were assembled inside a glove box full of high-purity argon. The galvanostatic charge–discharge was conducted on LAND battery program control test system (Wuhan, China) between 1.0 V and 3.5 V at the current densities of 50 and 100 mA $g^{-1}$. EIS measurements were performed on CHI660C electrochemical workstation using a three-electrode

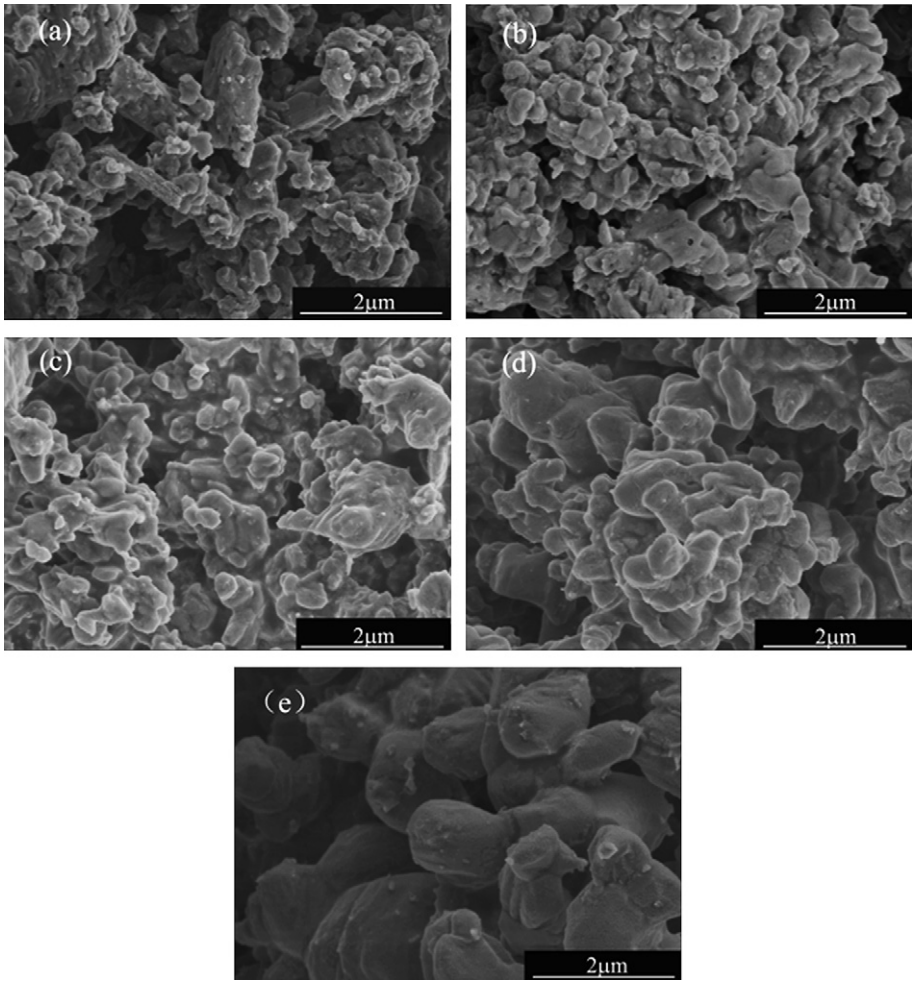


**Fig. 2.** SEM images of $LiVO_3$ synthesized at different temperatures: (a) 300 °C; (b) 350 °C; (c) 400 °C; (d) 450 °C; (e) 500 °C.

cell with the metallic lithium foil as both the reference and counter electrodes at discharge state. The amplitude of the AC signal was 5 mV over a frequency range from 100 kHz to 10 mHz. For GITT measurement, the LAND battery test system was programmed to supply a constant current flux (50 mA $g^{-1}$) for a given period (10 min) followed by an open-circuit stand of the cell for a specified time (40 min). This procedure was repeated for the full potential window of 1.0–3.5 V.

## 3. Results and discussion

The XRD patterns of the compounds prepared at different temperatures are shown in Fig. 1. Except the pattern of the product synthesized at 300 °C, all the other patterns are almost similar, and the diffraction peaks can be indexed to $LiVO_3$ phase (JCPDS card No. 70-1545) with C2/c space group. There is an impurity in the product synthesized at 300 °C, and the peak intensity of the impurity is as strong as the pure $LiVO_3$. It indicates that the reaction is not complete because of the low calcination temperature. When the calcination temperature is too high, there is possibility of decompose, so the pattern of product synthesized at 550 °C shows very weak peak of impurity. It is known that the diffusion paths of $Li^+$ in the materials with higher crystallization become longer [31], resulting in the poor electrochemical properties. In this work, the $LiVO_3$ synthesized at a low temperature has relatively low peak intensity which demonstrates low crystallization. It is expected that the $LiVO_3$ synthesized at the low temperature will exhibit good electrochemical performance. Fig. 2 shows the morphologies of the $LiVO_3$ powders synthesized at temperatures between 300 and 500 °C. The particle size of the $LiVO_3$ compound increases with the calcination temperature. The small particle size provides a short diffusion pathway for lithium ion insertion–extraction from host materials, together with high specific surface areas which can afford more active intercalation sites [32,33].

Fig. 3a shows the initial charge–discharge curves of the $LiVO_3$ electrodes between 1.0 and 3.5 V at room temperature. It can be seen that the shapes of the initial charge–discharge curves are almost the same. The $LiVO_3$ synthesized at 350 °C delivers an initial capacity of 302.5 mAh $g^{-1}$ at a current density of 50 mA $g^{-1}$, higher than those prepared at 300 °C (283.8 mAh $g^{-1}$), 400 °C (295.2 mAh $g^{-1}$), 450 °C (294.8 mAh $g^{-1}$), 500 °C (293.9 mAh $g^{-1}$) and 550 °C (227.9 mAh $g^{-1}$). Cycling performance of the $LiVO_3$ electrodes is displayed in Fig. 3b. The reversible charge–discharge process has a characteristic of solid solution [13], which results in good cyclic performance of the $LiVO_3$ electrodes. After 50 cycles, the $LiVO_3$ synthesized at 350 °C can still sustain a discharge capacity of 245.3 mAh $g^{-1}$ at a current density of 50 mA $g^{-1}$, showing good capacity retention. The cycling performance of the $LiVO_3$ synthesized at 550 °C is inferior to the others, which can be ascribed to its large particle size. While the poor cycling performance of the $LiVO_3$ synthesized at 300 °C results mainly from the impurity existence. Fig. 3c shows the cycling performance of the $LiVO_3$ electrodes at a current density of 100 mA $g^{-1}$, the compound synthesized at 350 °C also displays the best electrochemical performance. Fig. 3d shows the rate capability of the $LiVO_3$ synthesized at 350 °C between 1.0 and 3.5 V. At a low current density of 50 mA $g^{-1}$, the electrode delivers a high discharge capacity of 303.8 mAh $g^{-1}$. With the increase of current density, the discharge capacity decreases slightly. Nevertheless, even at a high current density of 800 mA $g^{-1}$, it can still deliver a discharge capacity of 161.5 mAh $g^{-1}$. As the current density is lowered to 50 mA $g^{-1}$, the discharge capacity can be recovered to 241 mAh $g^{-1}$, revealing good electrochemical reversibility. It is concluded that the $LiVO_3$ synthesized at a relatively low temperature has good electrochemical performances, which can be

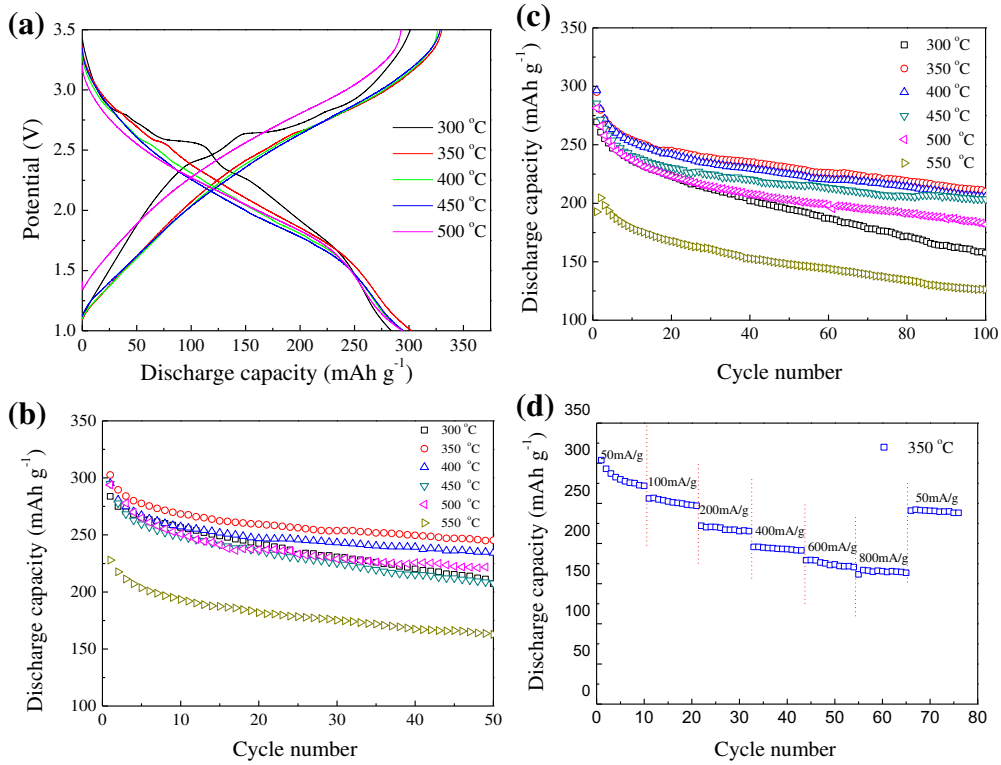


**Fig. 3.** (a) Initial charge–discharge curves, (b) cycling performance at a current density of 50 mA $g^{-1}$, (c) cycling performance at a current density of 100 mA $g^{-1}$, (d) rate capacity of the $LiVO_3$ synthesized at 350 °C at various charge–discharge current densities.

attributed to its relatively low crystallization and small particle size. The capacity fading of the compounds possibly results from the volume change and the dissolution of vanadium ions during charge–discharge cycling like some other vanadium derivatives [34–36].

Fig. 4 shows three-dimensional Nyquist plots for the $LiVO_3$ electrodes. The EIS were recorded at room temperature during the first to 100th charge–discharge cycles. The shapes of the Nyquist plots are all similar. The plots are consisted of three regions. The first part is an intercept at $Z'$ axis in high frequency, and the second part is a depressed semicircle in the middle frequency region, while the last part is the Warburg-type element (the sloping line) in the low frequency region. An intercept at $Z'$ axis in high frequency corresponds to the ohmic resistance of electrode. The depressed semicircle in the middle frequency range is attributed to the charge transfer resistance and the double layer capacitance. The low frequency Warburg impedance is corresponding mainly to the diffusion of $Li^+$ in the bulk electrode [37–40].

The impedance spectra are fitted using the equivalent circuit model, as shown in Fig. 5. $R_{ct}$ represents the charge transfer resistance of electrochemical reaction. $C_f$ and $R_f$ are the capacitance and resistance of solid electrolyte interface (SEI) films, respectively. $Q$ is associated with the capacitance of the double layer and passivation film. $W$ represents the diffusion-controlled Warburg impedance [41,42]. The intercept which corresponds to the ohmic resistance ($R_e$) is relatively small (about 10 Ω) for all the plots. The fitting results of $R_{ct}$ according to the equivalent circuit model are presented in Fig. 6. The higher the charge transfer resistance, the slower the kinetics of the cell reactions. As shown in Fig. 6, the compound synthesized at 350 °C has low values of $R_{ct}$, indicative of a faster kinetics in electrochemical reactions. The first $R_{ct}$ is 101.2 Ω, then it decreases to 10.3 Ω at the 10th cycle. After 100 cycles, it is still as

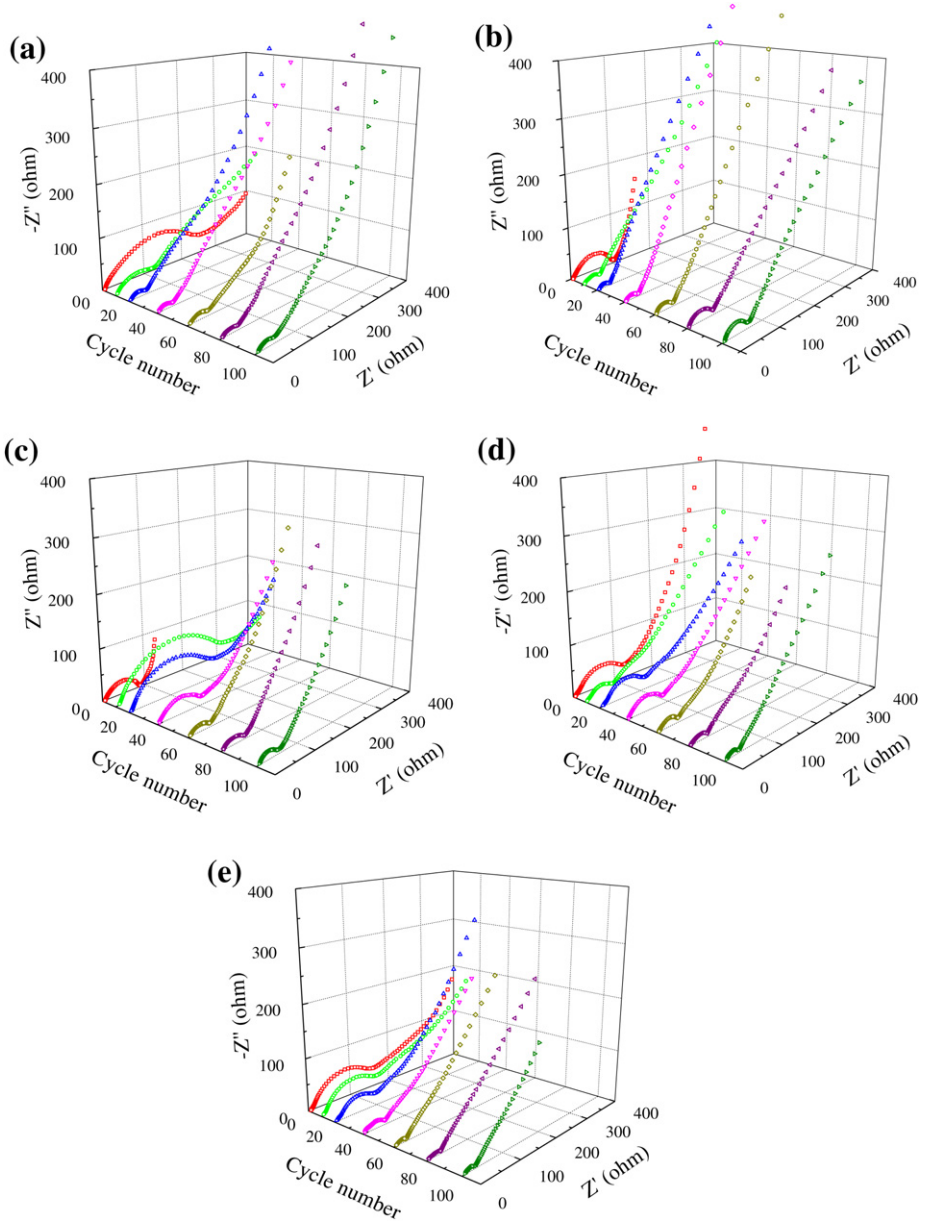


**Fig. 4.** Three-dimensional Nyquist plots measured after cycling for the $LiVO_3$ electrodes synthesized at different temperatures: (a) 300 °C; (b) 350 °C; (c) 400 °C; (d) 450 °C; (e) 500 °C.

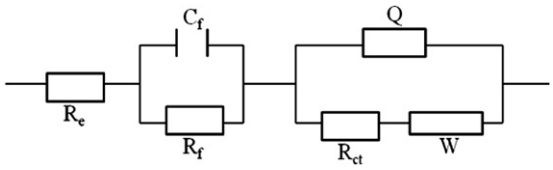


**Fig. 5.** The equivalent circuit model for $LiVO_3$ electrode.

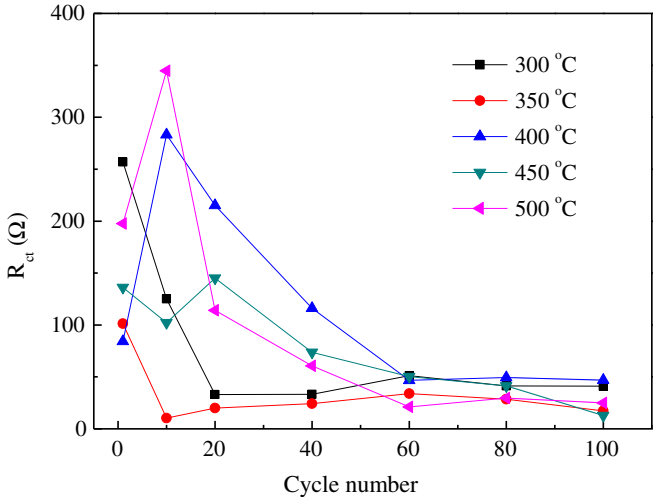


**Fig. 6.** Variation of $R_{ct}$ with cycling number calculated from fitting the Nyquist plots.

low as 17.4 Ω, which demonstrates that the polarization of the $LiVO_3$ electrode is extremely small.

GITT is one of the methods used to calculate the diffusion coefficient of $Li^+$ in electrodes. It has been widely used in lots of research works for its reliability [37,43,44]. Fig. 7a shows the GITT curves of the $LiVO_3$ electrode synthesized at 350 °C during the first cycle as a function of time in the voltage range of 1.0–3.5 V. The cell was first charged at a consent current flux ($I_0 = 50$ mA $g^{-1}$) for an interval of 10 min followed by an open-circuit stand for 40 min to allow the cell voltage to relax to its steady-state value ($E_s$). The applied current flux and the resulting potential profile for a single titration at the first charge state of 1.24 V is shown in Fig. 7b, with schematic labeling of different parameters, $\Delta E_\tau$, $\Delta E_s$, etc. The diffusion coefficient of $Li^+$ in the $LiVO_3$ electrode can be determined by solving Fick's second law of diffusion. After a series of assumptions and simplifications, the diffusion coefficient of $Li^+$ can be calculated by the following equation [45]:

$$D_{\mathrm{Li}} = \frac{4}{\pi}\left(\frac{m_B V_m}{M_B A}\right)^2 \left(\frac{\Delta E_s}{\tau\left(\frac{dE_\tau}{d\sqrt{\tau}}\right)}\right)^2 \quad \left(\tau << L^2/D_{\mathrm{Li}}\right) \tag{1}$$

where $V_m$ is the molar volume of the compound, $M_B$ is the molecular weight of the compound; $m_B$ and $L$ is the mass and the thickness of the electrode, respectively; $A$ is the interface between the active material and electrolyte.

If $E$ versus $\tau^{1/2}$ shows a straight line behavior during titration as shown in Fig. 7c, Equation (1) can be simplified as:

$$D_{\mathrm{Li}} = \frac{4}{\pi\tau}\left(\frac{m_B V_m}{M_B A}\right)^2 \left(\frac{\Delta E_s}{\Delta E_\tau}\right)^2 \tag{2}$$

According to Equation (2), we can calculate the diffusion coefficient of $Li^+$ from the GITT curves during both charge and discharge processes. The result is plotted in Fig. 7d. The values of $D_{Li^+}$ are in the range from $10^{-9.5}$ to $10^{-8}$ $cm^2$ $s^{-1}$ during the charge–discharge

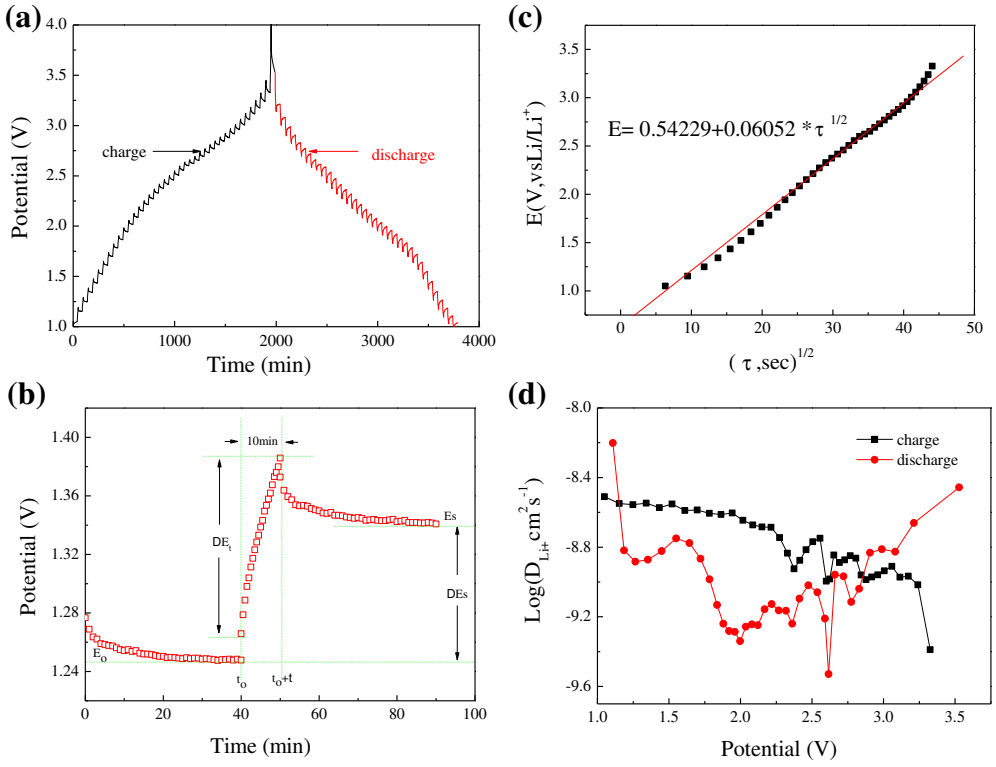


**Fig. 7.** (a) GITT curves of $LiVO_3$ electrode synthesized at 350 °C during the first cycle as a function of time in the potential range of 1.0–3.5 V; (b) $t$ vs. $E$ profile of $LiVO_3$ electrode for a single GITT titration at the charge state of 1.25 V; (c) plot of voltage against $\tau^{1/2}$ to show the linear fit; (d) the calculated $D_{Li^+}$ from the GITT data for the $LiVO_3$ electrode as a function of potential during charge and discharge processes.

processes. The diffusion coefficient of $Li^+$ for the $LiVO_3$ electrode is higher than that of some other cathodes, such as $Li_3V_2(PO_4)_3$ ($10^{-13}$–$10^{-8}$ $cm^2$ $s^{-1}$, GITT) [46], $LiFePO_4$ ($10^{-14}$–$10^{-11}$ $cm^2$ $s^{-1}$, GITT) [47], $LiV_3O_8$ ($10^{-14}$–$10^{-10}$ $cm^2$ $s^{-1}$, GITT) [36].

## 4. Conclusions

To summarize, pure $LiVO_3$ compound was synthesized at a relatively low temperature of 350 °C. Owing to its relatively low crystallization and small particle size, the $LiVO_3$ electrode displays optimal electrochemical performances, delivering a high discharge capacity of 302.5 mAh $g^{-1}$ between 1.0 and 3.5 V at a current density of 50 mA $g^{-1}$, and exhibiting good cyclic performance and small polarization. The diffusion coefficient of $Li^+$ in the $LiVO_3$ electrode calculated by GITT is in the range of $10^{-9.5}$–$10^{-8}$ $cm^2$ $s^{-1}$, which is higher than that of some other cathodes. The $LiVO_3$ compound is a promising cathode candidate for lithium ion batteries.

## Acknowledgments

This work was supported by the National Science and Technology Support Program (2012BAK30B04-05) and Key Science and Technology Innovation Team of Zhejiang Province (2010R50013).

## References

[1] H. Li, Z.X. Wang, L.Q. Chen, X.J. Huang, Adv. Mater. 21 (2009) 4593.
[2] L.F. Xiao, Y.Q. Zhao, Y.Y. Yang, Y.L. Cao, X.P. Ai, H.X. Yang, Electrochim. Acta 54 (2008) 545.
[3] S.C. Yin, H. Grondey, P. Strobel, H. Huang, L.F. Nazar, J. Am. Chem. Soc. 125 (2003) 326.
[4] L.Q. Mai, X. Xu, L. Xu, C.H. Han, Y.Z. Luo, J. Mater. Res. 26 (2011) 2175.
[5] P.L. Moss, R. Fu, G. Au, E.J. Plichta, Y. Xin, J.P. Zheng, J. Power Sources 124 (2003) 261.
[6] M. Vijayakumara, S. Selvasekarapandiana, R. Kesavamoorthy, K. Nakamurac, T. Kanashiro, Mater. Lett. 57 (2003) 3618.
[7] W.J. Wang, H.Y. Wang, S.Q. Liu, J.H. Huang, J. Solid State Electrochem. 16 (2012) 2555.
[8] D.A. Semenenko, D.M. Itkis, E.A. Pomerantseva, E.A. Goodilin, T.L. Kulova, A.M. Skundin, Y.D. Tretyakov, Electrochem. Commun. 12 (2010) 1154.
[9] Q. Shi, J.W. Liu, R.Z. Hu, M.Q. Zeng, M.J. Dai, M. Zhu, RSC Adv. 2 (2012) 7273.
[10] A. Sakunthala, M.V. Reddy, S. Selvasekarapandian, B.V.R. Chowdari, P.C. Selvin, J. Phys. Chem. C 114 (2010) 8099.
[11] C.Q. Feng, S.Y. Chew, Z.P. Guo, J.Z. Wang, H.K. Liu, J. Power Sources 174 (2007) 1095.
[12] Y.Q. Qiao, J.P. Tu, X.L. Wang, J. Zhang, Y.X. Yu, C.D. Gu, J. Phys. Chem. C 115 (2011) 25508.
[13] V. Pralong, V. Gopal, V. Caignaert, V. Duffort, B. Raveau, Chem. Mater. 24 (2012) 12.
[14] R.D. Shannon, C. Calvo, Can. J. Chem. 51 (1973) 265.
[15] C. Muller, J.C. Valmalette, J.L. Soubeyroux, F. Bouree, J.R. Gavarri, J. Solid State Chem. 156 (2001) 379.
[16] S. Selvasekarapandian, M. Vijayakumar, Solid State Ion. 148 (2002) 329.
[17] H.M. Liu, Y.G. Wang, K.X. Wang, Y.R. Wang, H.S. Zhou, J. Power Sources 192 (2009) 668.
[18] L. Liu, L.F. Jiao, J.L. Sun, M. Zhao, Y.H. Zhang, H.T. Yuan, Y.M. Wang, Solid State Ion. 178 (2008) 1756.
[19] X.Z. Ren, S.M. Hu, C. Shi, P.X. Zhang, Q.H. Yuan, J.H. Liu, J. Solid State Electrochem. 16 (2012) 2135.
[20] X.W. Zhou, G.M. Wu, G.H. Gao, C.J. Cui, H.Y. Yang, J. Shen, B. Zhou, Z.H. Zhang, Electrochim. Acta 74 (2012) 32.
[21] Y.X. Gu, D.R. Chen, X.L. Jiao, F.F. Liu, J. Mater. Chem. 16 (2006) 4361.
[22] Y.C. Si, L.F. Jiao, H.T. Yuan, H.X. Li, Y.M. Wang, J. Alloys. Compd. 486 (2009) 400.
[23] Y.L. Cheah, V. Aravindan, S. Madhavi, J. Electrochem. Soc. 159 (2012) A273.
[24] A. Subramania, N. Angayarkanni, S.N. Karthick, T. Vasudevan, Mater. Lett. 60 (2006) 3023.
[25] S.H. Ju, Y.C. Kang, Electrochim. Acta 55 (2010) 6088.
[26] X.H. Xiong, Z.X. Wang, H.J. Guo, X.H. Li, F.X. Wu, P. Yue, Electrochim. Acta 71 (2012) 206.
[27] T.J. Patey, S.H. Ng, R. Büchel, N. Tran, F. Krumeich, J. Wang, H.K. Liu, P. Novák, Electrochem. Solid-State Lett. 11 (2008) A46.
[28] X.W. Gao, J.Z. Wang, S.L. Chou, H.K. Liu, J. Power Sources 220 (2012) 47.
[29] Y.W. Wang, H.Y. Xu, H. Wang, Y.C. Zhang, Z.Q. Song, H. Yan, C.R. Wan, Solid State Ion. 167 (2004) 419.
[30] Y.Q. Qiao, X.L. Wang, J.P. Zhou, J. Zhang, C.D. Gu, J.P. Tu, J. Power Sources 198 (2012) 287.
[31] K. West, B. Zachau-Christiansen, S. Skaarup, Y. Saidi, J. Barker, I.I. Olsen, R. Pynenburg, R. Koksbang, J. Electrochem. Soc. 143 (1996) 820.
[32] H.W. Lee, P. Muralidharan, R. Ruffo, C.M. Mari, Y. Cui, D.K. Kim, Nano Lett. 10 (2010) 3852.
[33] X. Liu, J. Wang, J. Zhang, S. Yang, J. Mater. Sci. 42 (2007) 867.
[34] L.L. Liu, X.J. Wang, Y.S. Zhu, C.L. Hu, Y.P. Wu, R. Holze, J. Power Sources 224 (2013) 290.
[35] W. Tang, X.W. Gao, Y.S. Zhu, Yun.B. .Yue, Y. Shi, Y.P. Wu, K. Zhu, J. Mater. Chem. 22 (2012) 20143.
[36] A.Q. Pan, J. Liu, J.G. Zhang, G.Z. Cao, W. Xu, Z.M. Nie, X. Jie, D. Choi, B.W. Arey, C.M. Wang, S.Q. Liang, J. Mater. Chem. 21 (2011) 1153.
[37] Z. Li, F. Du, X.F. Bie, D. Zhang, Y.M. Cai, X.R. Cui, C.Z. Wang, G. Chen, Y.J. Wei, J. Phys. Chem. C 114 (2010) 22751.
[38] T. Jiang, W.C. Pan, J. Wang, X.F. Bie, F. Du, Y.J. Wei, C.Z. Wang, G. Chen, Electrochim. Acta 55 (2010) 3864.
[39] Y.Q. Qiao, J.P. Tu, X.L. Wang, C.D. Gu, J. Power Sources 199 (2012) 287.
[40] J.Y. Xiang, J.P. Tu, L. Zhang, X.L. Wang, Y. Zhou, Y.Q. Qiao, Y. Lu, J. Power Sources 195 (2010) 8331.
[41] X.P. Zhang, H.J. Guo, X.H. Li, Z.X. Wang, L. Wu, Electrochim. Acta 64 (2012) 65.
[42] Z.Y. Chen, C.S. Dai, G. Wu, M. Nelson, X.G. Hu, R.X. Zhang, J.S. Liu, J.C. Xia, Electrochim. Acta 55 (2010) 8595.
[43] K.M. Shaju, G.V.S. Rao, B.V.R. Chowdari, Electrochim. Acta 48 (2003) 2691.
[44] S.J. Shi, J.P. Tu, Y.Y. Tang, Y.X. Yu, Y.Q. Zhang, X.L. Wang, J. Power Sources 221 (2013) 300.
[45] W. Weppner, R.A. Huggins, J. Electrochem. Soc. 124 (1977) 1569.
[46] X.H. Rui, N. Ding, J. Liu, C. Li, C.H. Chen, Electrochim. Acta 55 (2010) 2384.
[47] W.L. Liu, J.P. Tu, Y.Q. Qiao, J.P. Zhou, S.J. Shi, X.L. Wang, C.D. Gu, J. Power Sources 196 (2011) 7728.